

Supplementary Information for

## **Electrochemically mediated ATRP in ionic liquids: Controlled polymerization of methyl acrylate in [BMIm][OTf]**

Francesco De Bon,<sup>a</sup> Marco Fantin,<sup>b</sup> Abdirisak Ahmed Isse,<sup>a,\*</sup> and Armando Gennaro<sup>a,\*</sup>

<sup>a</sup>Department of Chemical Sciences, University of Padova, via Marzolo 1, 35131 Padova, Italy

<sup>b</sup>Department of Chemistry, Carnegie Mellon University, 4400 Fifth Avenue, Pittsburgh, PA 15213, USA

### Table of Contents

S1. Experimental procedures	(2)
S2. Comparison of [BMIm][OTf] with acetonitrile	(3)
S3. Electrochemical characterization of [BMIm][OTf]	(3)
S4. Galvanostatic <i>e</i> ATRP	(4)
S5. Halogen exchange	(6)
S6. NMR of PMA- <i>b</i> -PAN	(8)
S7. Characterization of recycled ionic liquid	(9)

## S1. Experimental procedures

### S1.1. Activation of working electrodes

The platinum gauze used as the working electrode in *e*ATRP was initially cleaned electrochemically by applying a series of anodic/cathodic steps (10 cycles at  $-1$  A for 60 s and  $+1$  A for 120 s in a solution of  $\text{H}_2\text{O}/\text{H}_2\text{SO}_4/\text{HNO}_3$  1:1:1 v/v/v). Afterwards, before each *e*ATRP experiment, it was activated by cycling the potential between  $+0.7$  and  $-1$  V vs.  $\text{Hg}/\text{Hg}_2\text{SO}_4$  at  $0.2$  V/s (60 cycles) in  $0.5$  M aqueous  $\text{H}_2\text{SO}_4$ . The electrode was then rinsed with double distilled water and acetone. The glassy carbon disk used for CV analysis was initially polished with 1000, 2500 and 4000 grit silicon carbide papers, and 3-, 1-,  $0.25\text{-}\mu\text{m}$  diamond pastes. Each polishing step was followed by ultrasonic rinsing in ethanol for 5 min. Before each experiment, the electrode surface was refreshed by polishing with the  $0.25\text{-}\mu\text{m}$  diamond paste, followed by ultrasonic rinsing in ethanol.

### S1.2. Chain extension of poly(methyl acrylate)-Br with AN via catalytic halogen exchange

Once the desired conversion of MA was reached, the applied potential was switched to  $E_{\text{app}} = E_{1/2} + 0.20$  V to stop polymerization by converting  $\text{Cu}^{\text{I}}$  to  $\text{Cu}^{\text{II}}$  (deactivator) species. The temperature of the water jacket was then raised to  $75$  °C and the cell was fluxed with a vigorous flow of  $\text{N}_2$  for 10 min to eliminate the residual MA monomer. Then, after reducing the gas flux and disconnecting the water jacket,  $2.5$  mL of AN ( $38.2$  mmol) were introduced together with  $8.3$  mg of tetraethylammonium chloride ( $0.05$  mmol). The solution was then degassed for 10 min under a light flow of inert gas and the water jacket, thermostated at  $50$  °C, was connected. Cyclic voltammetry (CV) was recorded to calculate  $E_{1/2}$  of the newly formed  $[\text{Cl-CuTPMA}]^+$ . Chain extension was triggered by applying  $E_{\text{app}} = E_{1/2} - 0.06$  V.

### S1.3. Ionic liquid recycling and polymer recovery

At the end of polymerization, the temperature of the water jacket was raised to  $75$  °C and the cell was fluxed with a vigorous flow of  $\text{N}_2$  for 10 min to eliminate the residual monomer by evaporation. Then,  $3 \times 20$  mL extractions with toluene were performed to remove the polymer. At the end of the third extraction, the IL fraction was removed and treated at rotary evaporator at  $80$  °C for 20 min to remove traces of toluene. The recovered ionic liquid was further dried at  $110$  °C under vacuum ( $0.03$  mbar) for 20 min. The final yield of recovered IL was 90%. The combined toluene fractions, collected in a round bottom flask, yielded the polymer after evaporation at a rotavapor. The recovered polymer was 98% of the produced one, calculated on the monomer conversion basis.

## S2. Comparison of [BMIm][OTf] with acetonitrile

To compare IL with traditional molecular solvents, *e*ATRP was performed under the same experimental conditions in [BMIm][OTf] and in acetonitrile (MA/solvent = 1:1 (v/v),  $C_{\text{MA}}:C_{\text{Cu}}:C_{\text{TPMA}}:C_{\text{RX}} = 552:0.1:0.1:1$ , with  $C_{\text{Cu}} = 10^{-3}$  M). To increase the electric conductivity of acetonitrile, 0.1 M Et<sub>4</sub>NBF<sub>4</sub> was added as a supporting electrolyte. The chosen applied potential was  $E_{\text{app}} = E_{1/2} - 0.060$  V. The results are listed in Table S1.

Table S1. *e*ATRP of MA in CH<sub>3</sub>CN or IL at  $E_{\text{app}} = E_{1/2} - 0.060$  V.<sup>a</sup>

entry	solvent	<i>T</i> (°C)	<i>t</i> (h)	conv. (%)	$k_p^{\text{app, b}}$ (h <sup>-1</sup> )	<i>Q</i> (C)	$M_{n,\text{th}}$	$M_{n,\text{app}}$	<i>D</i>
1	CH <sub>3</sub> CN	25	4	92	0.62	3.49	43700	42700	1.14
2	[BMIm][OTf]	25	5	90	0.17	1.30	42800	42300	1.10
3	[BMIm][OTf]	50	1.75	93	1.52	3.00	44200	44200	1.17
4	CH <sub>3</sub> CN	50	2	93	1.31	5.39	47000	45000	1.09

<sup>a</sup>Other experimental conditions: 0.1 M Et<sub>4</sub>NBF<sub>4</sub> was used as a supporting electrolyte in CH<sub>3</sub>CN; estimated surface area of the working electrode: 6 cm<sup>2</sup>. <sup>b</sup>The slope of ln([M]<sub>0</sub>/[M]) vs. *t* plot.

Polymerizations of MA in [BMIm][OTf] and in acetonitrile were overall very similar in terms of molecular weights and dispersity. Polymerization rate in [BMIm][OTf] was significantly slower than in CH<sub>3</sub>CN at 25 °C, probably due to the much higher viscosity, and thus slower mass transport, in this solvent. At 50 °C similar reaction rates were observed, although dispersity was slightly lower in CH<sub>3</sub>CN than in the ionic liquid.

## S3. Electrochemical characterization of [BMIm][OTf]

Electrochemical characterization was carried out to evaluate electroactive impurities present in commercially available [BMIm][OTf]. Figure S1 shows background voltammograms recorded in [BMIm][OTf] before and after purification of the solvent. Various small peaks and a strong anticipation of the cathodic discharge is observed in the CV of the unpurified IL. The underlying redox processes may be due to residual water and other undesired impurities such as halide ions, which are typical byproducts of the synthesis of ionic liquids. After purification (see the main text), most electroactive impurities were removed as confirmed by the flat baseline recorded in the CV.

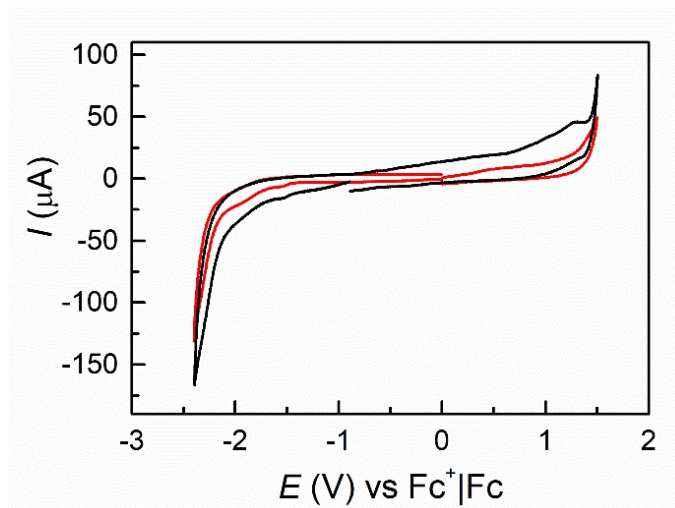


Figure S1. Cyclic voltammetry of pristine (—) and purified (—) [BMIm][OTf], recorded at 50 °C on a GC electrode at 0.2 V/s.

#### S4. Galvanostatic *e*ATRP

Switching from potentiostatic (fixed potential) to galvanostatic (fixed current) *e*ATRP has several advantages: i) the three-electrode system can be substituted with a two-electrode one (without a reference electrode); ii) a simple current generator can be used instead of a potentiostat; iii) the rate of  $\text{Cu}^{\text{I}}$  generation can be fixed and modulated by the applied current. Therefore, galvanostatic *e*ATRP was tested. The applied current,  $I_{\text{app}}$ , was chosen based on a chronoamperometry ( $i$  vs.  $t$ ) recorded during a potentiostatic *e*ATRP (Figure S2). Four current steps, with progressively decreasing  $I_{\text{app}}$ , were applied to simulate the variable rate of  $\text{Cu}^{\text{I}}$  production under potentiostatic conditions. The current steps were chosen to produce  $[\text{Cu}^{\text{I}}\text{L}]^+$  at a high rate at the beginning of the polymerization and then slowly in later stages of the process [1].

Applying a fixed current, instead of a fixed potential, causes the working electrode potential ( $E_{\text{WE}}$ ) to drift over time.  $E_{\text{WE}}$  was monitored during *e*ATRP, and its typical trend is reported in Figure S2b.  $E_{\text{WE}}$  shifted to more negative values during a fixed current polymerization step, but on average remained close to  $E_{\text{app}}$  used in the potentiostatic experiment ( $E_{\text{app}} = E_{1/2} - 0.060$  V). This allowed avoiding side reactions that occur at very negative potentials, such as electrodeposition of  $\text{Cu}^0$  on the working electrode. Figure S3 shows a comparison of *e*ATRP performed in potentiostatic or galvanostatic mode: the two experimental setup modes give substantially the same results in terms of both polymerization rate and properties of produced polymers.

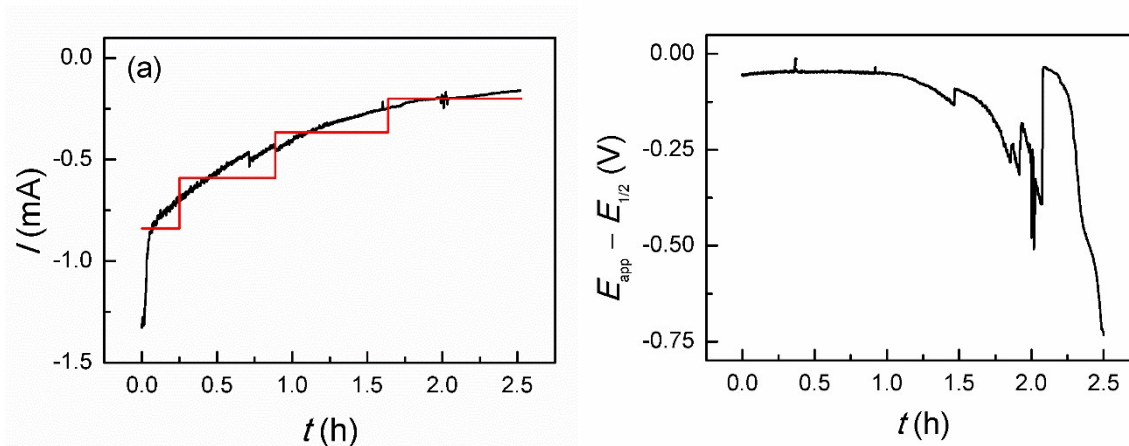


Figure S2. (a) Chronoamperometry recorded during potentiostatic *e*ATRP of MA in [BMIm][OTf] (1:1 v/v),  $T = 50\text{ }^{\circ}\text{C}$ ,  $E_{\text{app}} = E_{1/2} - 0.060\text{ V}$ ,  $C_{\text{MA}}:C_{\text{CuBr}_2}:C_{\text{TPMA}}:C_{\text{RX}} = 552:0.1:0.1:1$ ,  $C_{\text{CuBr}_2} = 10^{-3}\text{ M}$ ; the dotted line shows the fixed current steps applied in the galvanostatic mode. (b) Potential (vs.  $E_{1/2}$ ) of the working electrode during galvanostatic *e*ATRP.

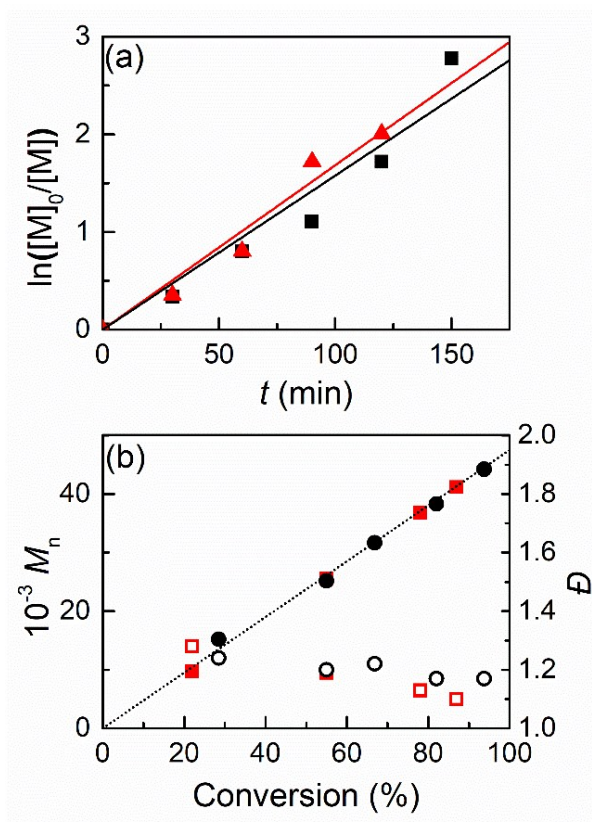


Figure S3. (a) Kinetic plot and (b) evolution of  $M_n$  and  $D$  as a function of conversion for potentiostatic *e*ATRP performed at  $E_{\text{app}} = E_{1/2} - 0.060\text{ V}$  (squares) and galvanostatic *e*ATRP (circles) at  $T = 50\text{ }^{\circ}\text{C}$ . Conditions:  $C_{\text{MA}}:C_{\text{CuBr}_2}:C_{\text{TPMA}}:C_{\text{RX}} = 552:0.1:0.1:1$ ,  $C_{\text{CuBr}_2} = 10^{-3}\text{ M}$ . The dotted line represents theoretical  $M_n$ .

## S5. Halogen exchange

At the end of a potentiostatic *e*ATRP of 50% (v/v) MA in [BMIm][OTf] the residual monomer was evaporated with a stream of nitrogen at 75 °C. Figure S4 shows <sup>1</sup>H NMR spectra of the reaction mixture before and after MA evaporation, confirming the complete removal of MA as evidenced by the disappearance of the signals of the olefinic protons of methyl acrylate ( $\delta = 5.8 - 6.4$  ppm).

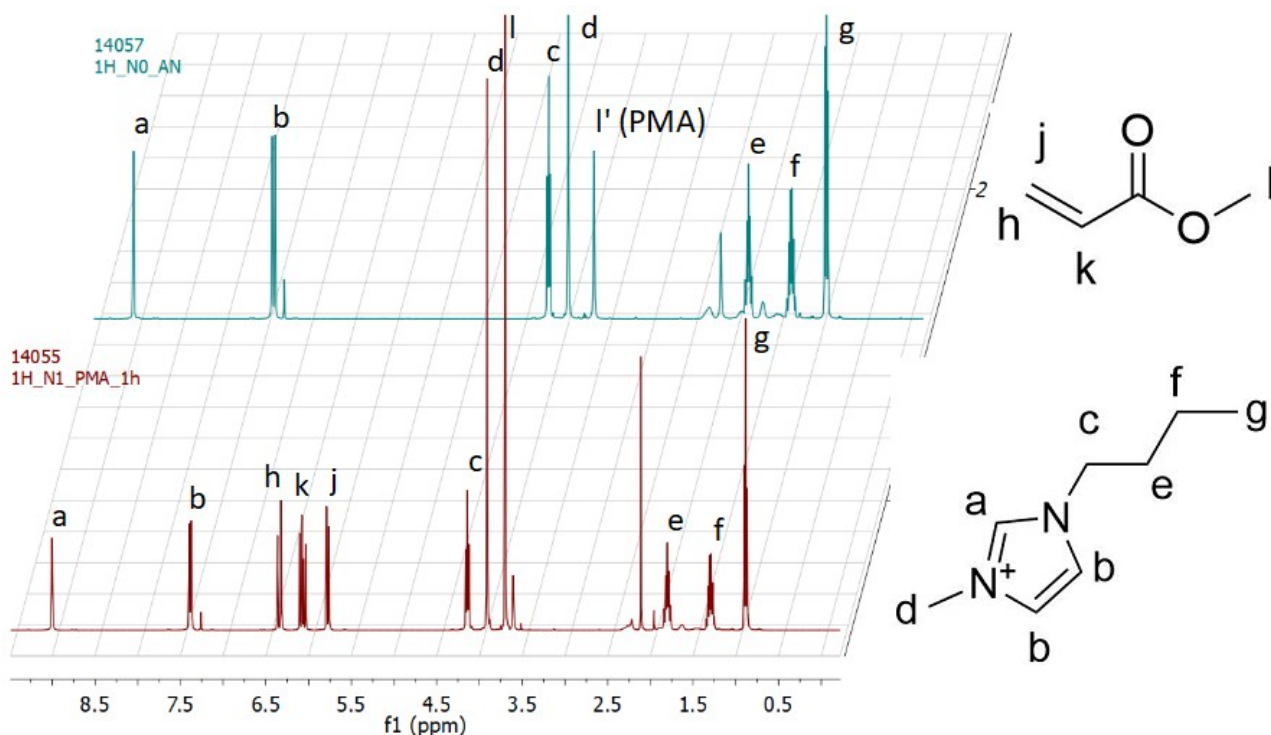


Figure S4. *e*ATRP of 50% (v/v) MA in [BMIm][OTf] performed at  $E_{\text{app}} = E_{1/2} - 0.060$  V. Conditions:  $C_{\text{MA}}:C_{\text{CuBr}_2}:C_{\text{TPMA}}:C_{\text{RX}} = 552:0.1:0.1:1$ ,  $C_{\text{CuBr}_2} = 10^{-3}$  M;  $T = 50$  °C. <sup>1</sup>H NMR spectra of the reaction mixture after 50% conversion, recorded before (—) and after the residual MA evaporation (—). No signals associated to olefinic protons were detected after removal of MA.

After evaporating the residual monomer, a reversible peak couple was observed in cyclic voltammetry, indicating the stability of the catalyst,  $[\text{BrCu}^{\text{II}}\text{TPMA}]^+$  in [BMIm][OTf]/PMA-Br ((73:27 w/w)). A voltammogram recorded immediately after addition of  $\text{Et}_4\text{NCl}$  showed complete disappearance of the peak couple of  $[\text{BrCu}^{\text{II}}\text{TPMA}]^+$ , which was replaced by a new peak couple attributed to  $[\text{ClCu}^{\text{II}}\text{TPMA}]^+$ . The following equilibria are established when  $\text{Cl}^-$  is added to a solution of  $[\text{BrCu}^{\text{II}}\text{TPMA}]^+$ :





If  $K_{\text{Cl}} \gg K_{\text{Br}}$ , as was previously observed for copper complexes of the same family in acetonitrile [2],  $[\text{ClCu}^{\text{II}}\text{TPMA}]^+$  will be quantitatively formed by substitution of  $\text{Br}^-$  by  $\text{Cl}^-$ . The observed disappearance of the peak couple of  $[\text{BrCu}^{\text{II}}\text{TPMA}]^+$  confirms that the bromide complex is no longer present in solution. The clean shift of redox potential to more negative values agrees with the electrochemical behavior of Cu catalysts previously studied in  $[\text{BMIm}][\text{OTf}]$  [3]. Also,  $E_{1/2}$  of the new species agrees well with the standard potential of  $[\text{ClCu}^{\text{II}}\text{TPMA}]^+$  in  $[\text{BMIm}][\text{OTf}]$  [3].

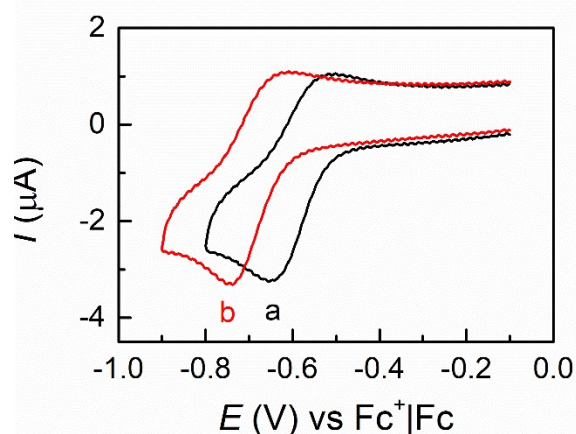


Figure S5. Cyclic voltammetry of 0.001 M  $[\text{BrCu}^{\text{II}}\text{TPMA}]^+$  in  $[\text{BMIm}][\text{OTf}]/\text{PMA-Br}$  ((73:27 w/w), after *e*ATRP of 50% (v/v) MA and evaporation of residual monomer, recorded at  $\nu = 0.2$  V/s in the absence (a) and presence (b) of 0.012 M  $\text{Et}_4\text{NCl}$ .

To confirm that equilibria (1) and (2) strongly favor  $[\text{ClCu}^{\text{II}}\text{TPMA}]^+$  over the bromide complex, another exchange experiment was performed in  $[\text{BMIm}][\text{OTf}]$ . A solution of 0.0011 M  $[\text{ClCu}^{\text{II}}\text{TPMA}]^+$  was prepared in  $[\text{BMIm}][\text{OTf}]$  by dissolving equimolar amounts of  $\text{CuCl}_2$  and TPMA. As reported previously [3], cyclic voltammetry of this solution showed a reversible peak couple due to the reversible one-electron reduction of  $[\text{ClCu}^{\text{II}}\text{TPMA}]^+$  to  $[\text{ClCu}^{\text{I}}\text{TPMA}]$  (Fig. S6). Addition of 0.012  $\text{Et}_4\text{NBr}$  did not significantly affect the voltammetric pattern of the system, which remained essentially the same as that of the  $[\text{ClCu}^{\text{II}}\text{TPMA}]^+ / [\text{ClCu}^{\text{I}}\text{TPMA}]$  couple. If  $\text{Br}^-$  exchange with  $\text{Cl}^-$  were favored, a reversible peak couple with  $E_{1/2} = -0.62$  V vs  $\text{Fc}^+/\text{Fc}$  would have appeared after bromide addition. No such a peak couple was observed in the presence of excess  $\text{Br}^-$ , clearly indicating that  $[\text{ClCu}^{\text{II}}\text{TPMA}]^+$  is much more stable than  $[\text{BrCu}^{\text{II}}\text{TPMA}]^+$ ; the arrow in Fig. S6 indicates the position of the missing peak couple to be attributed  $[\text{BrCu}^{\text{II}}\text{TPMA}]^+$ .

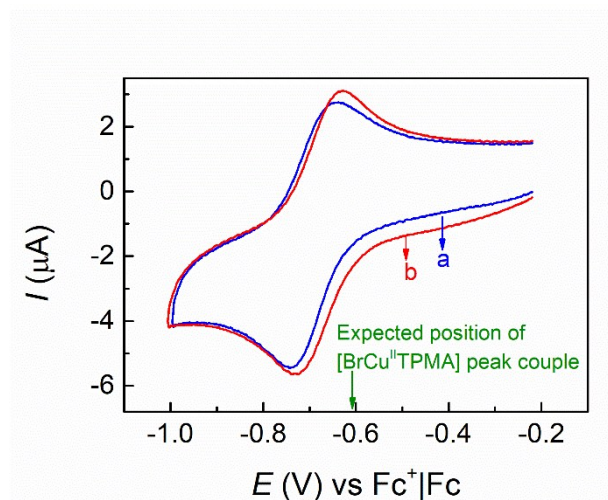


Figure S6. Cyclic voltammetry of 0.0011 M  $[\text{ClCu}^{\text{II}}\text{TPMA}]^+$  in pure  $[\text{BMIm}][\text{OTf}]$ , recorded at  $\nu = 0.2$  V/s in the absence (a) and presence (b) of 0.012 M  $\text{Et}_4\text{NBr}$ .

### S6. NMR of PMA-*b*-PAN

At the end of the chain extension experiment, the polymer poly(methyl acrylate)-*b*-poly(acrylonitrile)-Cl was precipitated in water, washed with methanol and dried under high vacuum for several hours. NMR analysis of the isolated polymer (Fig. S7) confirmed the presence of both poly(methyl acrylate) and polyacrylonitrile blocks.

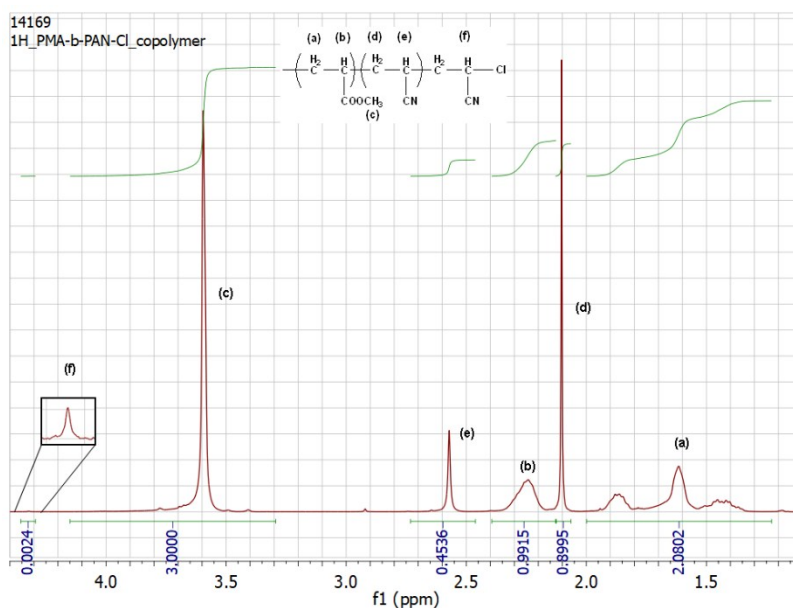


Figure S7.  $^1\text{H}$  NMR spectrum of extracted and precipitated poly(methyl acrylate)-*b*-poly(acrylonitrile)-Cl. Relevant peaks have been integrated and associated as indicated in the figure.



## S7. Characterization of recycled ionic liquid and recovered PMA-Br

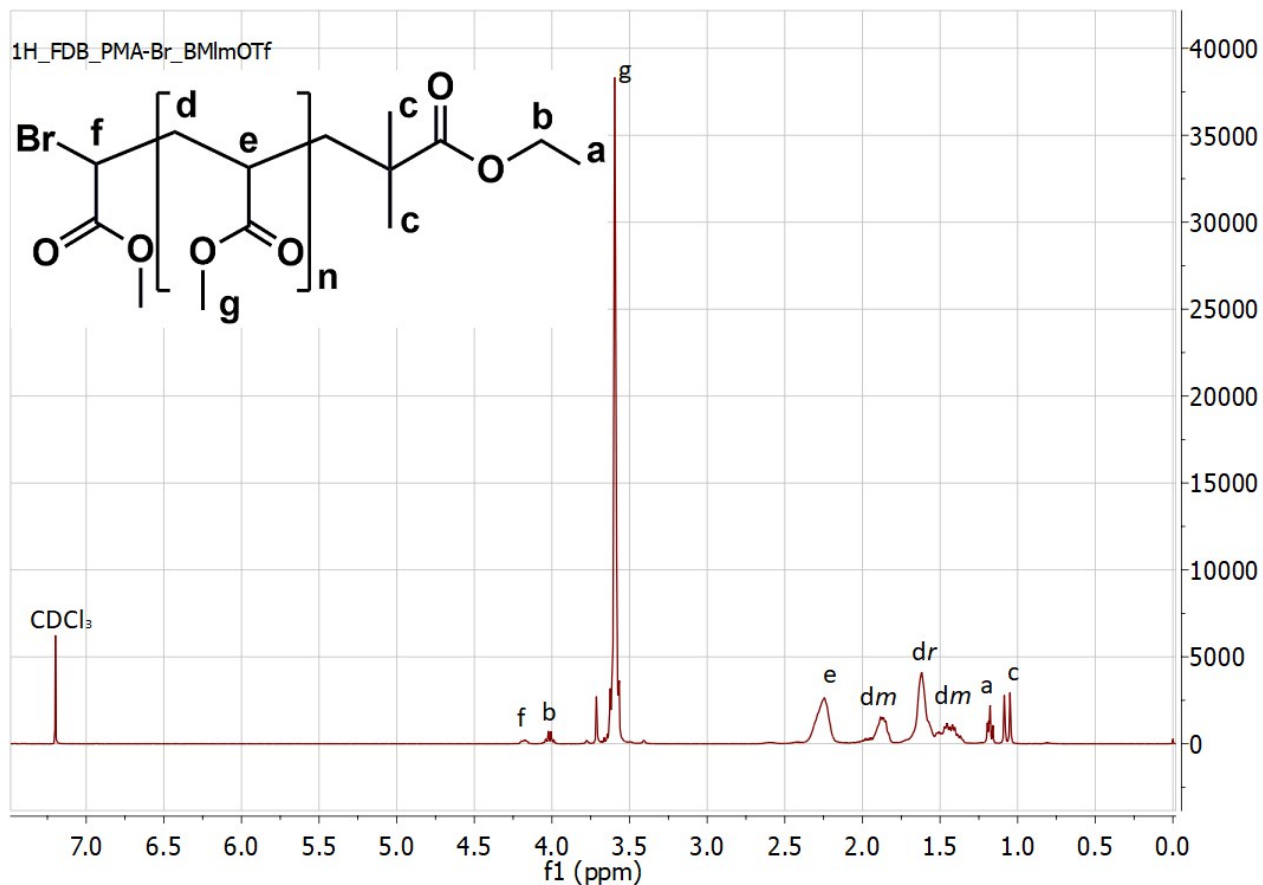


Figure S8. <sup>1</sup>H NMR spectrum of poly(methyl acrylate)-Br after extraction with toluene.

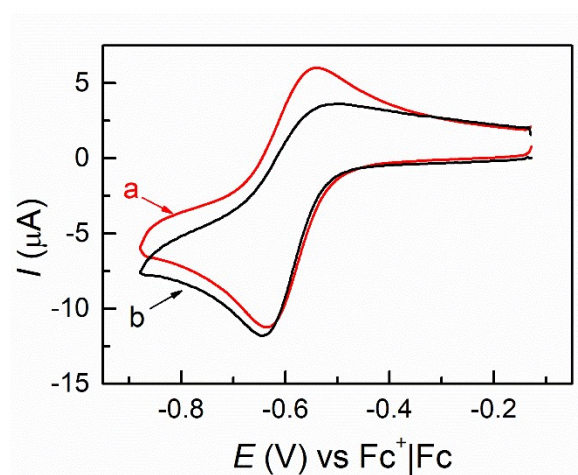


Figure S9. Cyclic Voltammetry of  $10^{-3}$  M  $[\text{Br-Cu}^{\text{II}}\text{TPMA}]^+$  in 50% (v/v) MA in (a) fresh  $[\text{BMIm}][\text{OTf}]$  or (b) residual IL after *e*ATRP followed by extraction of the polymer in toluene, recorded at 25 °C on a GC electrode at 0.2 V/s.

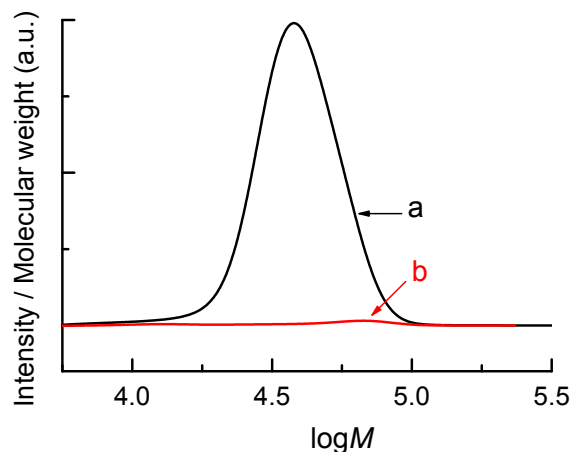


Figure S10. GPC chromatograms of recovered [BMIm][OTf] before (a) and after (b) the polymer extraction.

## References

- [1] F. Lorandi, M. Fantin, A.A. Isse, A. Gennaro, Electrochemically mediated atom transfer radical polymerization of *n*-butyl acrylate on non-platinum cathodes, *Polym. Chem.* 7 (2016) 5357–5365.
- [2] N. Bortolamei, A.A. Isse, V. B. Di Marco, A. Gennaro, K. Matyjaszewski, Thermodynamic properties of copper complexes used as catalysts in atom transfer radical polymerization, *Macromolecules*, 43 (2010) 9257-9267.
- [3] F. Lorandi, F. De Bon, M. Fantin, A.A. Isse, A. Gennaro, Electrochemical characterization of common catalysts and initiators for atom transfer radical polymerization in [BMIm][OTf], *Electrochem. Commun.* 77 (2017) 116–119.